Transitions in Boundary Layer Meso-γ Convective Structures: An Observational Case Study

DAVID A. R. KRISTOVICH AND NEIL F. LAIRD

Atmospheric Environment Section, Illinois State Water Survey, Champaign, Illinois

MARK R. HJELMFELT, RUSSELL G. DERICKSON, AND KEVIN A. COOPER

Institute for Atmospheric Sciences, South Dakota School of Mines and Technology, Rapid City, South Dakota

(Manuscript received 13 April 1998, in final form 16 October 1998)

ABSTRACT

Boundary layer rolls over Lake Michigan have been observed in wintertime conditions predicted by many past studies to favor nonroll convective structures (such as disorganized convection or cellular convection). This study examines mechanisms that gave rise to transitions between boundary layer rolls and more cellular convective structures observed during a lake-effect snow event over Lake Michigan on 17 December 1983. The purposes of this study are to better understand roll formation in marine boundary layers strongly heated from below and examine the evolution of snowfall rate and mass overturning rate within the boundary layer during periods of convective transition. A method of quantifying the uniformity of convection along the roll axes, based on dual-Doppler radar-derived vertical motions, was developed to quantify changes in boundary layer convective structure. Roll formation was found to occur after (within 1 h) increases in low-level wind speeds and speed shear primarily below about $0.3z_i$, with little change in directional shear within the convective boundary layer. Roll convective patterns appeared to initiate upstream of the sample region, rather than form locally near the downwind shore of Lake Michigan. These findings suggest that either rolls developed over the upwind half of Lake Michigan or that the convection had a delayed response to changes in the atmospheric surface and wind forcing. Mass overturning rates at midlevels in the boundary layer peaked when rolls were dominant and gradually decreased when cellular convection became more prevalent. Radar-estimated aerial-mean snowfall rates showed little relationship with changes in convective structure. However, when rolls were dominant, the heaviest snow was more concentrated in updraft regions than during more cellular time periods.

1. Introduction

Lake-effect snow and rainstorms contribute significantly to the total wintertime precipitation in the Great Lakes region (e.g., Eichenlaub 1979; Braham and Dungey 1995; Scott and Huff 1996; Miner and Fritsch 1997). Snowfall patterns around the western Great Lakes reveal that as the mean west to northwesterly winds blow across these lakes, lake-effect precipitation concentrates along the downwind (eastern) shoreline regions (Braham and Dungey 1984). Kelly (1986) and Kristovich and Steve (1995) found that the most common convective pattern over all of the Great Lakes, particularly Lakes Superior, Michigan, and Huron, is widespread fields of snow associated with winds across the short axis of the lakes. These widespread cloud and precipitation fields, observed by satellite and WSR-88D radars, usually exhibit multiple wind-parallel banded features. Kelly (1984) and Kristovich (1993) used single- and dual-Doppler radar observations near the eastern shore of Lake Michigan to show that roll vortices were present when the convective pattern was organized into wind-parallel bands of heavier precipitation.

Numerous investigators have examined roll development in various environmental conditions. Some notable reviews of published research on boundary layers and roll convection can be found in Kelly (1977), Etling and Brown (1993), Moeng and LeMone (1995), and Atkinson and Zhang (1996). In general, past research emphasized that under conditions of weak to moderate thermal forcing from the surface, convection tended to organize into longitudinal roll convection when winds and wind shear were high (e.g., Woodcock 1940; Grossman 1982). Current roll formation theories emphasize the importance of the curvature of wind speed profiles parallel to the roll axes (e.g., Kuettner 1959, 1971), inflection points in the wind speed profiles perpendicular to the roll axes (e.g., Brown 1970, 1972, 1980), and boundary layer mean wind shear (Asai 1970, 1972; Miu-

Corresponding author address: Dr. David A. R. Kristovich, Illinois State Water Survey, 2204 Griffith Dr., Champaign, IL 61820-7495. E-mail: dkristo@uiuc.edu

ra 1986). Clark et al. (1986), Kuettner et al. (1987), and Hauf and Clark (1989) found that gravity waves, generated within the stable air above the convective boundary layer by wind shear near the boundary layer top, can augment linear convective structures. If the boundary layer top wind shear is roughly perpendicular to the boundary layer wind direction, then bands of convection parallel to the mean boundary layer wind can be induced by gravity waves. Rao and Agee (1996) and Cooper (1998) used numerical modeling techniques to determine that cloud microphysical processes and shear profiles influence the development of roll and nonroll convective patterns in lake-effect boundary layers. Kristovich (1993) compared atmospheric characteristics shown by the earlier studies to favor roll development over nonroll convection, with those observed on four dates with roll circulations over Lake Michigan. He found that none of the existing criteria for roll occurrence were met on all dates and suggested that low-level shear (below about 200-m height) was primarily responsible for roll development.

The purpose of this observational study is to gain a better understanding of mechanisms responsible for roll occurrence in boundary layers strongly heated from below. The temporal evolution of convection between nonroll and roll patterns and the changes in atmospheric conditions responsible for the transitions are examined for a lake-effect event that occurred on 17 December 1983. The term *nonroll* denotes nonlinear convective structures with high reflectivity and updraft centers with roughly the same size and spacing as the rolls. Section 2 gives an overview of studies of roll convection. Sections 3 and 4 describe the dataset and analysis methods used, including those for determining the convective uniformity along the roll axes. Sections 5 and 6 describe the evolution of synoptic conditions, mesoscale convective structure, and the internal boundary layer on 17 December 1983. Section 7 examines changes in snowfall and vertical mass overturning rates as the convective structure evolved. Finally, section 8 discusses and summarizes the findings of this study.

2. Background

A number of past studies give quantitative descriptions of environmental conditions that resulted in roll development, which can be compared to conditions observed in this case. For example, Brown (1972) argued that shear induced by a wind profile that turns with height, leaving an inflection point at midlevels, may be sufficient to overcome the stability profile in the atmosphere. When the magnitude of shear at the inflection point was sufficient to overcome the atmospheric stability (defined as the Richardson number near the height of the inflection point, Ri_L, was less than 0.25), then linear convective patterns were predicted. Miura (1986) found that rolls were favored when boundary layer wind shear was between 10^{-3} and 10^{-2} s^{-1}. Kuettner (1971) found that rolls existed when the alongroll wind profile curvature exceeded a value of 10^{-7} cm^{-1} s^{-1} over the depth of the boundary layer. Two different approaches employ ratios of the influence of shear and buoyancy on boundary layer turbulence. Grossman (1982), using theoretical arguments and observations of cloud bands taken during the Barbados Oceanographic and Meteorological Experiment, found evidence for roll convection or a combination of rolls and cells in vertical velocity measurements when the negative ratio of the boundary layer depth (z_i) to the Monin–Obukhov length (L, defined later) was greater than 21.4. Using numerical experiments, Sykes and Henn (1989) revealed that rolls developed when the ratio of the friction velocity (u_*) to the convective velocity scale (w_*) was greater than 0.35. Other factors, such as latent heat release by cloud and precipitation formation (e.g., Brümmer 1985; Sykes et al. 1988; Cooper 1998), are also thought to influence convective structures. The literature gives examples where the presence of clouds and precipitation favors nonroll convective structures (e.g., Brümmer 1985; Cooper 1998) or increases the likelihood of rolls (e.g., Sykes et al. 1988; Rao and Agee 1996).

Recent observational studies have shown that rolls can form in boundary layers more strongly heated from below than suggested by the above studies. On four wintertime lake-effect roll cases examined by Kristovich (1993), all with strong surface heating, none of the criteria shown by past authors to favor roll development were consistently met. However, the criteria for Kuettner (1971) was met when using wind shear below about $0.2z_i$. Kristovich (1993) concluded that near-surface shear was likely responsible for roll formation. This finding is similar to that by Sykes and Henn (1989), who used numerical modeling techniques to determine that shear close to the surface organizes convection at those levels into wind-parallel bands. This convection then rises through the remainder of the near-neutrally buoyant convective boundary layer, while retaining its linear pattern. Similarly, Weckwerth et al. (1997) used observed and numerically derived turbulent kinetic energy calculations to show that wind shear close to the surface was more important than shear throughout the boundary layer in sustaining roll convection observed over east-central Florida during the Convection and Precipitation/Electrification Experiment (CaPE). In general, however, the CaPE studies examined cases with low wind speeds and weak to moderate heating from the surface. The present study examines the evolution of convective structures between rolls and nonroll convection within a boundary layer strongly heated from below. Our goal is to gain further insight into the forcing mechanisms responsible for roll occurrence in highly convective boundary layers.

It is well known that convective rolls modulate boundary layer turbulent eddies (e.g., LeMone 1973, 1976; Grossman 1982), clouds (e.g., Kuettner 1959; Streten 1975; LeMone and Pennell 1976), and precip-

itation (Kelly 1984; Rao and Agee 1996). Much less is known, however, about the possible relationships between the rate of mass overturning and the organization of convection within the boundary layer. Braham (1986) observed a case when transitions between nonroll and roll convection were accompanied by large changes in the spatial coverage of snowfall and perhaps the mean snowfall rate. This study examines how mass overturning rates, snowfall rates, and boundary layer depth respond to changes in both surface forcing and the structure of mesoscale convection.

3. Data and analysis approach

Data used for the analysis of the 17 December 1983 lake-effect snow event were taken during the University of Chicago Lake-Effect Snow Storm Project that was conducted during December 1983 and January 1984. This field project included dual-Doppler radar measurements, aircraft in situ observations (NCAR *King Air* and *Queen Air*), research rawinsonde observations of atmospheric profiles, and Portable Automated Mesonet surface stations (see Schoenberger 1986). Atmospheric conditions, including convective boundary layer depth and wind profiles, were derived from surface, radar, rawinsonde, and aircraft observations. The National Centers for Environmental Prediction global tropospheric gridded analysis maintained by the National Center for Atmospheric Research (NCAR) was used for examining the synoptic evolution of this event.

The primary dataset used in this study was taken by the NCAR *CP3* and *CP4* 5-cm wavelength radars, which provided dual-Doppler coverage near the east (downwind) shore of Lake Michigan (Fig. 1). Radar scans were generally taken between 0.0° or 0.1° and about 5.0° elevation angle, with a vertical resolution of generally 0.4° or 0.5°. The radar equivalent reflectivity factor (hereafter called reflectivity) and radial velocity fields were interpolated to a Cartesian grid using the NCAR Mesoscale and Microscale Meteorology Division (MMM) Sorted Position Radar Interpolation program (Mohr and Vaughan 1979; Miller et al. 1986). The primary analysis region was 25 km × 25 km with horizontal and vertical grid spacings of 250 m and 200 m, respectively. It is noted that over portions of the sample region, data between height levels is not independent. Tests using vertical grid spacings between 200 and 350 m revealed only minor changes in calculated vertical velocity fields. All heights presented in this paper (unless otherwise noted) are relative to the surface. The analysis region was large enough to include several roll wavelengths during periods of boundary layer roll convection.

Dual-Doppler syntheses of the horizontal winds, calculation of derived fields, and creation of graphical displays of the data were done with the NCAR MMM Custom Editing and Display of Reduced Information in Cartesian Space program (Mohr et al. 1986). In addition,

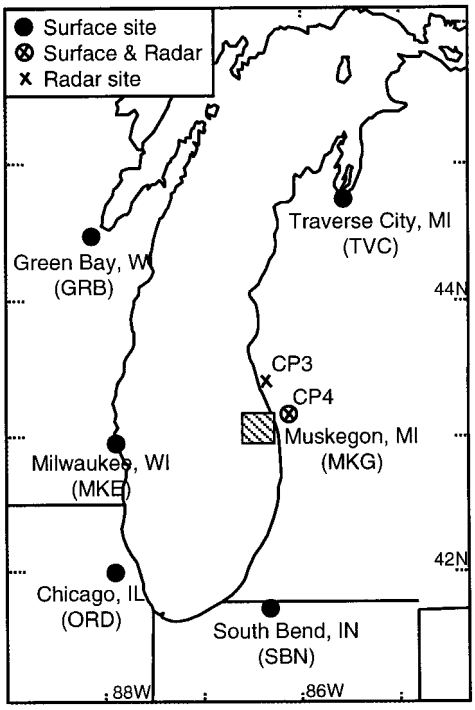

FIG. 1. Map showing locations of National Weather Service surface observational sites and NCAR *CP3* and *CP4* radars during the University of Chicago Lake-Effect Snow study. Radar analysis region is depicted by the hatched square.

the NCAR MMM Planned Position Indicator program was used to examine the radar measurements at the original sampling resolution throughout a larger region over the lake (55 km × 50 km). Vertical motions were calculated using observed convergence fields, and integrating the continuity equation downward from an altitude of 1100 m (the height of the top of the boundary layer near the eastern shore). Use of a single value for boundary layer top height is justified because of the observed small variations in the cloud tops (e.g., Chang and Braham 1991; Braham and Kristovich 1996) and intense above–boundary layer stability. Variational or bottom-up methods appeared to be less reliable in this case due to the shallow nature of the convective circulations and the radar ranges required to observe them with ground-based radars in Michigan.

Six surface stations that provided meteorological parameters along the eastern and western shores of Lake Michigan were used in estimating surface fluxes (Fig. 1). Measurements of Lake Michigan surface water temperature, from Coast Guard observations and aircraft downward-looking radiometer observations, ranged from 2° to 5°C. Due to uncertainty of the representativeness of the lake water temperatures, and the fact that a small amount of floating ice was observed from the aircraft, a water temperature of 0°C was used in estimating the heat and moisture fluxes. This may have resulted in underestimates of the surface heat, momen-

tum, and moisture fluxes. However, temporal trends of the fluxes should be well represented. Heat and moisture fluxes were estimated using bulk methods every hour along the western and eastern shores during the lake-effect event, using

$$H = c_p C_H \rho u(\theta_{\mathrm{LM}} - \theta) \Rightarrow H = c_p C_H \rho u(T_{\mathrm{LM}} - T), \quad (1)$$

$$E = C_E \rho u(q_{\mathrm{LM}} - q) \Rightarrow E = C_E u(\rho_{v\text{-LM}} - \rho_v), \quad (2)$$

where H is sensible heat flux (W m^{-2}); E is vapor flux (g m^{-2} s^{-1}); C_H and C_E are nondimensional bulk transfer coefficients of heat and moisture, respectively; c_p is specific heat at constant pressure for air; ρ is air density; ρ_v is water vapor density; u is near-surface wind speed; θ is potential temperature; T is temperature; and q is specific humidity. The subscript LM denotes values associated with the surface of Lake Michigan. For this study, a value of 1004.5 J kg^{-1} K^{-1} was used for c_p and a constant value of 1.5×10^{-3} was used for C_H and C_E.

Several methods are available for comparing the influences of shear to buoyancy on boundary layer circulations. One of the most commonly used factors in the literature on roll formation is the negative ratio of the boundary layer depth (z_i) to the Monin–Obukhov length, L (e.g., Grossman 1982). This length is a measure of the ratio of shear to buoyant production of turbulent kinetic energy in the boundary layer and was estimated for this study by

$$-L = \frac{\rho C_p T u_*^3}{K_a g H\left(1 + \dfrac{0.07}{B}\right)}, \quad (3)$$

where the friction velocity is

$$u_* = [C_D u]^2 \quad (4)$$

with a constant drag coefficient, C_D, of 1.5×10^{-3} (Arya 1988, p. 160, 167, 171). For this calculation, u was assumed to be zero at the surface. The Bowen ratio, B, is the ratio of the surface sensible heat flux (H) to surface latent heat flux (E). Another common method of comparing shear to buoyant production is the ratio of the friction velocity (u_*) to the convective velocity scale, w_*, calculated here by

$$w_* = \left[\frac{g z_i\left(\dfrac{H}{\rho}\right)}{T}\right]^{1/3}. \quad (5)$$

Bulk transfer relationships were utilized for all flux calculations since vertical profile information was not available at each measurement location (Garratt 1992) and aircraft flight patterns on 17 December 1983 did not allow for determination of temporal variations in low-level fluxes. In utilizing the bulk transfer method, temporal trends in estimated and actual values of fluxes over Lake Michigan should be closely related, even though specific values may not be numerically equivalent. There are a variety of methods for estimating surface fluxes (e.g., Sykes et al. 1993). The methods used for this investigation were chosen because they give reasonable values compared to past aircraft observations of fluxes derived through eddy-correlation techniques in lake-effect situations (e.g., Chang and Braham 1991; Kristovich 1993; Kristovich and Braham 1998) and due to the limited vertical extent (i.e., measured at a single altitude) of the wind and temperature observations.

Wind shear at various levels was derived using single- and dual-Doppler radar data, project rawinsonde soundings from Muskegon, Michigan, about 10–15 km to the east of the dual-Doppler sample region, and wind profiles taken during aircraft takeoffs and landings.

4. Methods of determining degrees of linearity/cellularity

In this section, we combine a method employed by Weckwerth et al. (1997) with a new method of calculating the degree of convective uniformity along the roll axes based on vertical motion observations, so that changes can be quantitatively described. Observations of the radar reflectivity and radar-derived vertical motion fields on 17 December indicate that a gradual transition occurred between nonroll convection and horizontal roll circulations during a 5-h time period. The gradual transition of convective structure and meteorological conditions suggest that the differing convective modes existed simultaneously during this event. For example, linear convection (rolls) tended to dominate over nonroll convection between about 1510 and 1600 UTC. Nonroll convective elements remained during this time period, but to a lesser degree. The 17 December 1983 event provides an example of situations in which the transition between convective modes is gradual and difficult to define. Therefore, a method of quantifying the degree that linear and nonroll convection exist, especially under transitional time periods, is necessary.

Weckwerth et al. (1997) employed an autocorrelation technique to examine statistical properties of atmospheric bandedness within radar reflectivity fields observed during CaPE and model-derived vertical velocity fields. Spatial correlation fields allow for determination of regular, repeated patterns in a region of observed radar reflectivity (or other quantity). Weckwerth et al. (1997) used spatial autocorrelation fields to calculate a horizontal aspect ratio (HAR), which is a measure of the major axis versus the minor axis of the 0.2 correlation coefficient contour about the center of an autocorrelation field. Weckwerth et al. (1997) used HAR values of greater than six to identify the existence of rolls based on the visual inspection of many cases. It is not known if this criteria is appropriate for events with differing environmental conditions or radar scatterers, or in conditions where there is a spatial variation in roll

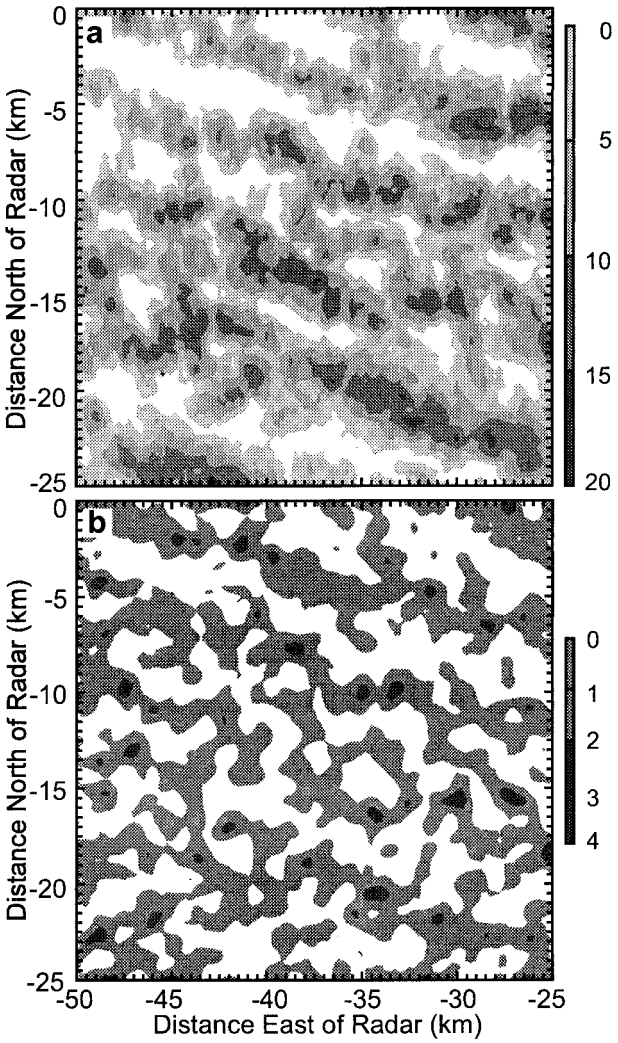

FIG. 2. Plan view of (a) radar reflectivity (dBZ) and (b) vertical motion (m s^{-1}) fields estimated from dual-Doppler radar horizontal wind observations at 1541 UTC 17 Dec 1983 at 700 m.

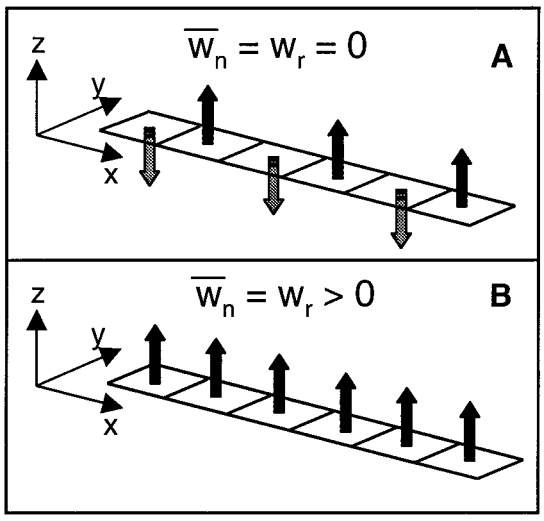

FIG. 3. Schematic illustration of the mass flux ratio (MFR) method for determining the uniformity of convection along boundary layer rolls. Case A represents one in which there is no roll-mean vertical motion field (i.e., mass flux due to rolls = 0); MFR = 0. Case B is one in which convection along the roll axes is uniform; MFR = 1.

wavelength (as seen in Muira 1986; Kelly 1984; Steve 1996).

An important assumption for the HAR method is that the reflectivity field is a reliable indicator of the vertical motion field, as has been indicated for convective boundary layers over land by Wilson et al. (1994). Figure 2 shows vertical motion estimates and radar reflectivity values for 1540 UTC on 17 December 1983. There is considerable agreement between these fields, particularly in regions of highest reflectivity and strongest vertical motions. However, the reflectivity field appears to be more coherent along the roll axes than the vertical motion field, where numerous downdrafts were located along the roll updraft axes. The presence of significant downdrafts along the roll updraft axes was shown using aircraft vertical motion and dual-Doppler radar observations by Kelly (1984) and Kristovich (1991, 1993). The more linear patterns in the reflectivity field may be due to the combined influences of snow formation everywhere in the cloud-filled upper boundary layer (Kristovich 1991) and the slow fall speeds of snow crystals (up to about 1 m s^{-1}). It is suggested that in order to fully understand the evolution of boundary layer convection, methods using both reflectivity and vertical motion fields are necessary.

Rather than rely entirely on reflectivity signatures, an alternative method of estimating linearity of roll convection was developed. This method utilizes measurements of mass flux, derived using radar-synthesized vertical wind fields, and is based on the dynamic structure of boundary layer roll circulations. As an illustration, consider the motions along a band of high reflectivity. Past observations reveal that the mean vertical motion along these high-reflectivity lake-effect bands is positive (Kelly 1984; Kristovich 1993). Superimposed on this weak mean upward vertical motion are stronger updrafts and downdrafts (Fig. 3). If synoptic-scale vertical motions are assumed to be negligible, then the vertical motion at a point (n) along the band (w_n) is the sum of the mean vertical motion along the strip ($\overline{w_n}$) and variation from the mean (w_n'); $w_n = \overline{w}_n + w_n'$. If the vertical motion is averaged along a sufficiently long strip, then nonroll motions would average to zero ($w_n' = 0$) and the average would represent the mean roll motion ($\overline{w}_n = w_R$). Therefore, the convective component at any location along the high-reflectivity band is simply $w_C = w_n - w_R$. For the 17 December 1983 case, mean roll vertical motions were estimated by calculating $[\Sigma_{n=1}^{k} (w_n)]/k$, where k is the number of samples within each 250-m-wide, 25-km-long strip parallel to the roll axes.

To derive a measure of convective uniformity along

the roll axes, it is convenient to use mass fluxes rather than vertical motions. The mass flux (F) at a point is $F_n = \rho w_n$. The mass flux due to the roll circulation at a given point in the high-reflectivity band is $F_{R_n} = \rho w_R$, since w_R is the same at all points in the high-reflectivity band. The total mass flux due to the roll-mean circulation was found by computing the sum of the roll mass fluxes at each point, $F_R = \sum_{n=1}^{k} F_{R_n} = k\rho w_R$. The total upward mass flux (F_T) was found by computing the sum of mass fluxes at all points with upward vertical velocities along the high-reflectivity band (i.e., $w_n > 0$). The ratio of mass flux due to the roll updraft to the mass flux due to all updrafts along the high-reflectivity band

$$\text{MFR} = F_R/F_T \tag{6}$$

is a measure of the uniformity of the roll circulations. Hereafter we will refer to this ratio as the mass flux ratio (MFR). If the vertical motion along a high-reflectivity band is uniform, then $F_R = F_T$, and MFR is unity (panel B in Fig. 3). For decreasing values of MFR, the vertical motions along the roll axes are more and more cellular. If the value of MFR is zero, then there is no roll updraft present (Fig. 3a). The same method can be applied to the roll-downdraft regions between high-reflectivity bands.

In lake-effect situations, Kelly (1984) and Kristovich (1993) found that bands of high reflectivity were associated with the updraft branch of roll circulations. Similar to Weckwerth et al. (1997), the correlation of bands of high reflectivity with the roll updrafts allow the orientation of roll axes to be determined using the major axis of the 0.2 contour from the spatial autocorrelation analyses of reflectivity. The orientation was easily determined during times with clearly definable linear patterns in the reflectivity field. Analyses were conducted for times when rolls existed (e.g., 1541 UTC) to determine the sensitivity of the MFR method to the roll orientation. Figure 4a shows that varying the roll orientation from 284°, the angle used to determine the MFR at 1541 UTC, by approximately 5° will result in about a 20% and 10% reduction of the MFR within the roll updrafts and downdrafts, respectively. Although relatively small variations in the orientation angle result in a significant error, the spatial autocorrelation method is best at determining the roll orientation angle when a high degree of linearity exists in the reflectivity field, as is the case when rolls are present.

The orientation angle is more difficult to define during periods of predominantly cellular convection. However, the MFR is less dependent on the determination of the orientation angle during these times due to the more random locations of the convective updrafts. Figure 4b shows the MFR as a function of orientation angle during a time when cellular convection existed (1502 UTC). Nearly all values of MFR are within 20% of the mean value (0.3). The values of MFR calculated using the orientation of 270°, determined by the spatial autocorrelation method, are within 10% of the mean. Also, values of MFR calculated using the mean wind direction at 700 m determined from dual-Doppler analysis (~280°) are also within 10% of the mean.

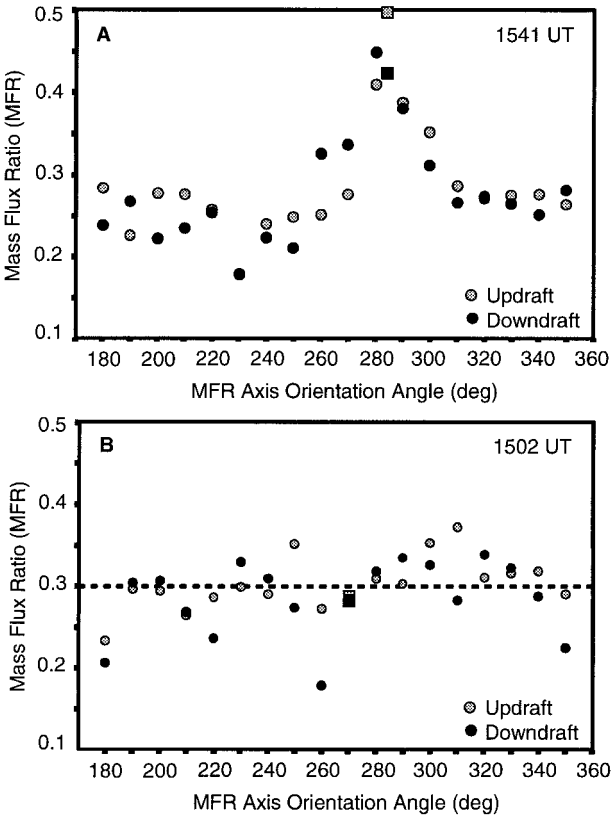

FIG. 4. MFR values as functions of geographic orientation angle for time periods with (a) rolls and (b) more cellular or random convective structure.

For this study, the spatial autocorrelation method was used to determine the roll orientation angle. When no angle was evident, the mean boundary layer wind direction was used. This angle was then employed to calculate the mass flux ratio.

5. Synoptic and meso-γ evolution on 17 December 1983

From 16–18 December 1983, the synoptic environment was dominated by a long-wave trough over the eastern United States that induced strong cold air advection over the Great Lakes region. At the surface, an anticyclone center moved southward from north of Lake Superior/Minnesota during the day on 16 December, across the Wisconsin/Illinois area on the morning of 17 December, to a position near Lake Huron by 0000 UTC 18 December. Minimum surface temperatures near the center of the cold pool decreased from about −27° to −31°C from 1200 UTC on 16 December to 1200 UTC on 18 December, with the coldest air moving from southern Manitoba, Canada, to southern Lake Michigan during this time period.

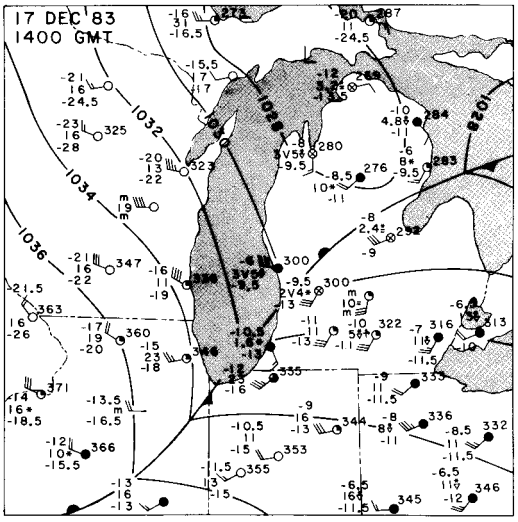

FIG. 5. Surface analysis for 1400 UTC on 17 Dec 1983. Wind barbs are in m s^{-1} with a full barb representing 2 m s^{-1}.

Surface observations in the western Great Lakes region (Fig. 5) reveal that a cold front moved through the Milwaukee, Wisconsin, area between 1300 and 1400 UTC on 17 December 1983, crossed southern Lake Michigan, and reached the MKG area between 1400 and 1500 UTC. Frontal passage over southern Lake Michigan was accompanied by an increase in surface and radar-measured wind speeds. MKG wind speeds increased from about 5–6 m s^{-1} before frontal passage to about 8–9 m s^{-1} after frontal passage, and radar-measured wind speeds at $0.7z_i$ (700 m) height increased from about 10 to 11 m s^{-1} during this time period. Wind directions were generally from the west, with a minor (10°–20°) shift toward more northerly winds after cold frontal passage. Thereafter, wind speeds slowly decreased with little change in wind direction throughout the rest of the observational period. At $0.7z_i$ (700 m) height, radar-synthesized winds decreased from about 11.2 m s^{-1} at 1500 UTC to approximately 10.4 m s^{-1} by around 1630 UTC. Thereafter, the wind speed remained nearly constant to about 1800 UTC. Wind speeds below 500 m, as estimated by aircraft and radar VAD analyses, changed more than those at higher levels in the boundary layer. Wind directions, however, were nearly unidirectional.

While the wind speed variations were small through much of the boundary layer, the variations were apparently strong enough to influence the structure of boundary layer convection observed near the eastern shore of Lake Michigan. Figure 6 gives the radar reflectivity pattern interpolated to the 700-m height level within the 625 km^2 dual-Doppler observational area. At 1409 UTC, before the cold frontal passage, there was little evidence of linear patterns in the reflectivity field, and the magnitude of the observed reflectivity was generally below 10 dBZ. After the cold frontal passage and as-

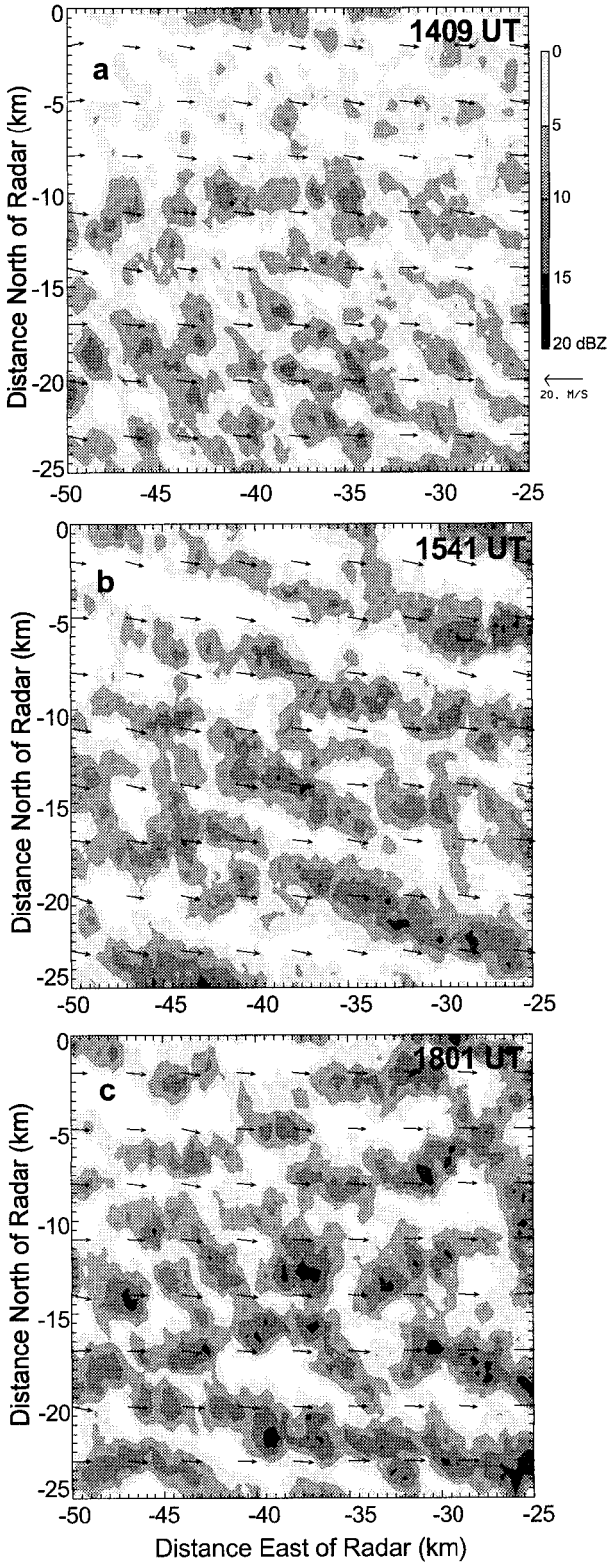

FIG. 6. Plan view of radar-measured effective reflectivity factor on 17 Dec 1983 at (a) 1409 UTC, (b) 1541 UTC, and (c) 1801 UTC. Reflectivity values and wind barbs shown are for the 700-m height level.

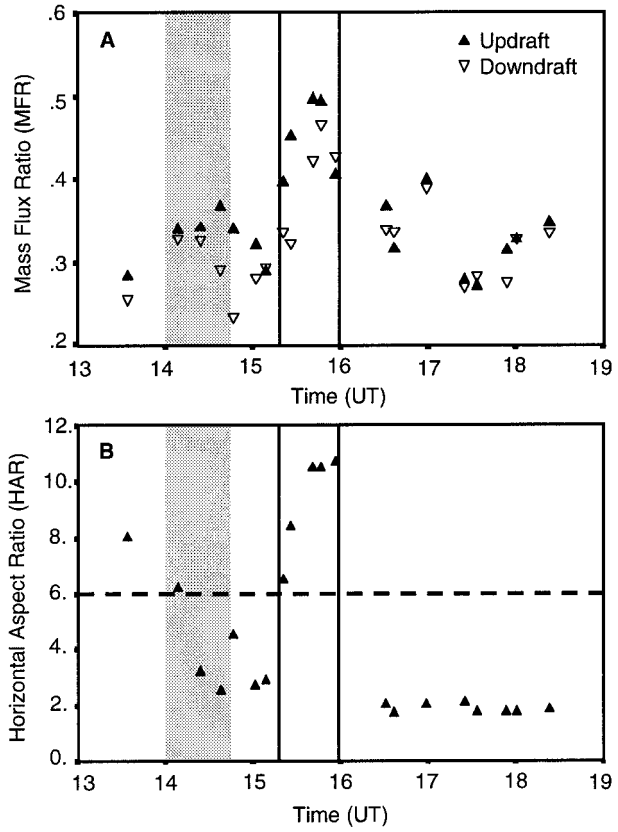

FIG. 7. Time series of MFR and HAR (see Weckwerth et al. 1997) on 17 Dec 1983. The approximate time of frontal passage in the sample region is shown as the dark gray vertical column. The time period where rolls were most dominant in the observed convective structure is shown in the white vertical column. (b) The horizontal line denotes the criteria above which Weckwerth et al. (1997) argued roll convection was present.

sociated peak in mean boundary layer wind speeds, linear patterns became much more pronounced, with wavelengths of 5–6 km (aspect ratios of about 5–6z_i). Peak magnitudes of reflectivity also increased, with reflectivities commonly over 10 dBZ in bands nearly parallel to the wind direction. As the winds thereafter decreased, the linear patterns became less prominent, with nonroll convective patterns becoming more pronounced. At 1801 UTC (panel C, Fig. 6), for example, wind-parallel bands of higher reflectivity can still be seen within the reflectivity field, but the lines are less coherent than at 1541 UTC.

Figure 7 gives a time series of values calculated by the HAR and MFR methods for estimating the degree of linearity within the observed convective field. These calculations utilized 20 radar volumes collected over a 5-h time period on 17 December 1983. Following a brief period of high HAR values (Fig. 7b), based on radar reflectivity patterns, values dropped below three. However, during the period between about 1510 UTC and 1600 UTC, HAR values were consistently larger (between about 6 and 11), with values above the minimum value defined by Weckwerth et al. (1997) as indicating roll convection during CaPE. Although the HAR values for the two earliest radar volumes (values of 8 and 6.2) are greater than the roll criterion used by Weckwerth et al. (1997), orientation angles of the reflectivity patterns were not close to the wind directions and apparently not due to longitudinal roll circulations.

Using radar-derived vertical motion fields at midlevels in the boundary layer, MFR values showed a similar pattern (Fig. 7a). Between about 1510 and 1600 UTC, when bands were most prominent in the reflectivity field, MFR values peaked in both the roll updraft and roll downdraft regions at about 0.50 and 0.46, respectively. These values indicate that during the period where the convection was most linear, roll-mean vertical motions accounted for about half of the total amount of updraft (downdraft) mass flux along the roll updraft (downdraft) region. After 1600 UTC, linear features became less prevalent and MFR values dropped to about 0.30—indicating that local updrafts along the roll axes had significantly increased. This suggests that during this time, the roll-mean circulations accounted for only about 30% of the total vertical motion along the bands.

6. Evolution of boundary layer structure

To better understand why the convective structure changed with time near the downwind shore, it is necessary to determine changes in atmospheric conditions that accompanied the evolution of convection. Past studies have emphasized the important roles of surface heating and wind shear within and just above the boundary layer in controlling the likelihood of roll or cellular convection. In this section, we will examine temporal and spatial changes in the atmospheric boundary layer on 17 December 1983.

a. Boundary layer changes across Lake Michigan

The west–east growth of the convective boundary layer was observed by the *King Air* and *Queen Air*, which conducted multiple vertical soundings within and above the boundary layer at locations across Lake Michigan. These observations were taken after frontal passage (*King Air* soundings were taken between 1517 and 1746 UTC, and *Queen Air* soundings were between 1632 and 1841 UTC). Because these data were taken over a period of several hours, these profiles may not be appropriate for a given instant of time. However, they do provide general information on the postfrontal thermal and microphysical characteristics of the convective boundary layer in which the convective transitions occurred. Figure 8 gives vertical cross sections across the lake of potential temperature, and the frequency with which clouds and snow were observed. For each 1-min flight segment, the potential temperature was averaged and plotted at the midpoint of the aircraft position. Cloud frequencies were determined for each flight seg-

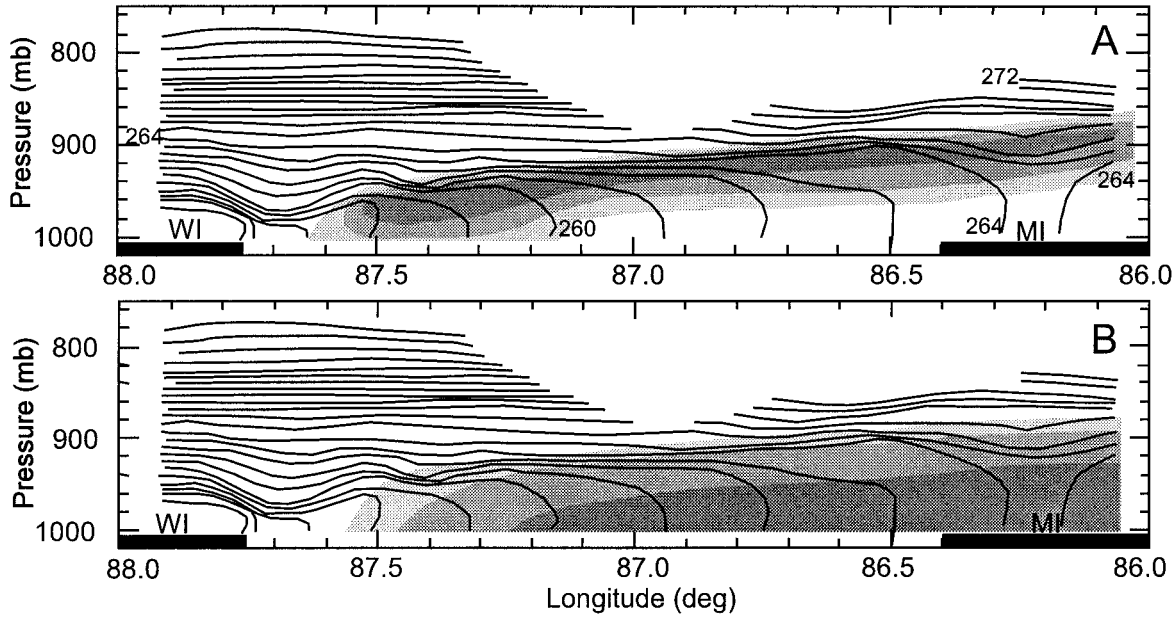

FIG. 8. Cross-lake cross sections of potential temperature (solid lines), and the percentage of 1-s samples that project aircraft encountered (a) clouds and (b) snow in each 1-min interval of flight. Potential temperatures are given every 1 K. Clouds were defined as having FSSP-measured concentrations over 10 cm^{-3}. Snow was having 200Y-measured concentrations over 0.1 L^{-1}. Gray shading represents locations where 20%, 60%, and 100% of each 1-min sample period has cloud or snow.

ment by tabulating the number of seconds with the Particle Measuring Systems Forward Scattering Spectrometer Probe (FSSP)-measured cloud drop particle concentrations over 10 cm^{-3} (Fig. 8a). The curves shown were subjectively drawn according to these data. Similarly, the snow frequencies represent the percent of seconds in the flight segments with 200Y-probe-measured snowflake concentrations over 0.1 L^{-1} (Fig. 8b).

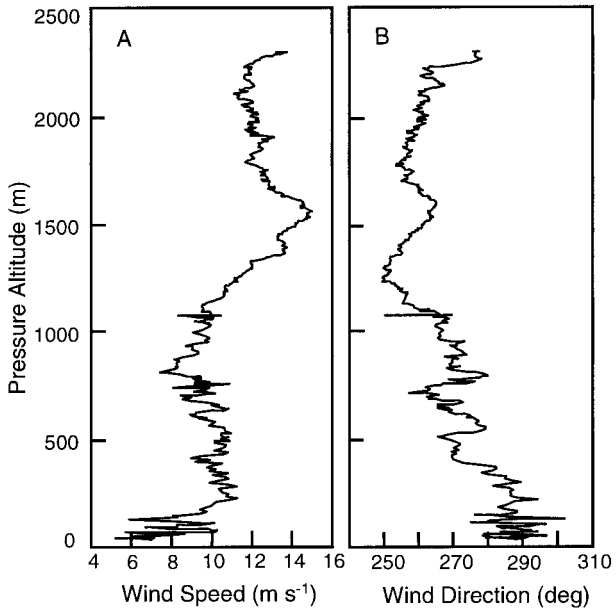

FIG. 9. Wind speed and direction profiles observed by the NCAR *King Air* during takeoff from Muskegon Airport (near 1516 UTC) on 17 Dec 1983.

The cross sections show that a convectively driven mixed layer grew with fetch across the lake into the stably stratified air. The boundary layer was neutral through most of the depth, with a very unstable surface layer near the lake (lake temperatures were estimated as between 0° and 3°C, 273 to 276 K). On this date, the boundary layer depth reached approximately 1.0 km near the downwind shore, giving an average slope of the boundary layer top across the lake of 8.3 m km^{-1}, over a fetch of about 120 km. A 200- to 600-m deep layer of nearly complete cloud coverage was observed across much of the lake and snow was observed nearly everywhere in the lower two-thirds of the boundary layer. It is important to note that the potential temperature gradient upwind of the lake was near 9 K km^{-1}, which would strongly inhibit vertical motions. Therefore, it seems likely that convective structures observed near the downwind shore were generated over the lake.

Aircraft-measured wind profiles taken during soundings over the lake (not shown) provided only general information due to the large amount of scatter in the data. Figure 9 shows an example aircraft profile taken at MKG near the downwind shore. All soundings over the lake revealed a rapid increase in wind speed from the surface to about 300-m height (Kristovich 1991). Between this height and about 900 m, wind speeds reached a local minimum. Above about 1000 m, wind speeds again increased rapidly. The wind direction varied by less than 25° so wind shear was roughly parallel

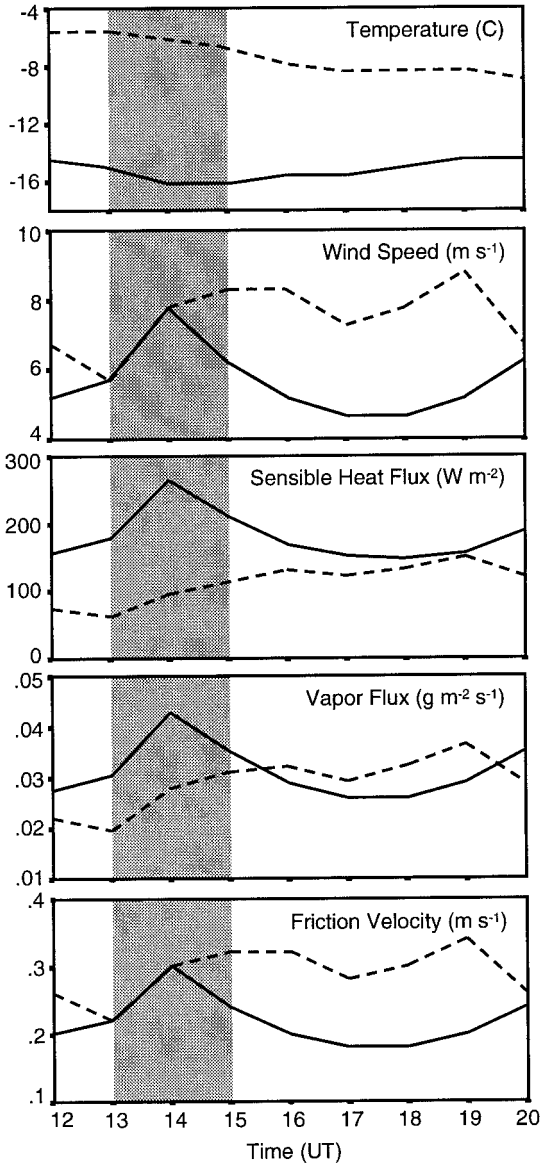

FIG. 10. Time series of surface observations of temperature, wind speed, and estimated overlake sensible heat flux, vapor flux, and friction velocity using surface observations taken at Milwaukee, WI (solid lines), and Muskegon, MI (dashed lines). Lake surface temperatures are assumed to be 0°C.

to the wind direction throughout the boundary layer. The strongest speed shear in the boundary layer was within the lowest 200–300-m height in all soundings. The difference between the low-level wind speed maximum and higher-level wind speed minimum decreased from west to east across the lake.

b. Temporal changes of surface fluxes

Temporal changes in surface fluxes were examined at six sites close to the lake (Fig. 1). Figure 10 gives time series of surface temperature and winds at Muskegan, MI (MKG) and Milwaukee, Wisconsin (MKE). Additionally, estimated surface heat and vapor fluxes, and friction velocity over the lake using near-shore surface measurements are shown. Temporal trends observed at four other sites around the lake showed similar variations. Trends in surface conditions were consistent with the passage of a cold front at around 1300–1500 UTC and a subsequent increase in wind speeds. There is some evidence for a second weak frontal passage after the time of dual-Doppler radar observations, around 2000–2200 UTC, after radar operations were terminated. Wind velocities at MKE underwent a spike in wind speeds of about 8 m s^{-1} at 1400 UTC, followed by a decrease in winds thereafter. This pattern is similar to those observed at Green Bay, Wisconsin, and Chicago, Illinois. Wind speeds near the downwind shore of the lake, illustrated by the observations at Muskegon, indicated generally increasing wind speeds with peaks of about 9 m s^{-1} at 1500–1600 UTC and around 1900 UTC.

Estimated surface sensible heat fluxes peaked at around 260–280 W m^{-2} near the upwind shore of Lake Michigan, and about 100 W m^{-2} lower near the eastern shore due to the lake-warmed surface air temperatures. Latent heat fluxes showed similar trends, but were much lower in magnitude (Bowen ratios were generally 2 to 3 near the upwind shore of the lake, and 1 to 2 near the downwind shore). Current theories generally suggest that for rolls to form, shear would have to offset these peak values of surface heat fluxes (e.g., Kuettner 1959, 1971; LeMone 1973; Grossman 1982; Sykes and Henn 1989; Etling and Brown 1993; Moeng and LeMone 1995; Atkinson and Zhang 1996). Indeed, friction velocities increased as heat fluxes increased and tended to have much higher values on the eastern side of the lake.

A measure of the ratio of shear to buoyant production of boundary layer motions, the Monin–Obukhov length (L), revealed that shear tended to contribute the most to turbulence formation just after frontal passage on 17 December 1983 (not shown), corresponding to the time periods of increases in surface heat flux. This is not surprising, given that the shear component in the numerator of the equation for L [Eqs. (3) and (4)] is a function of u^6, while the heat flux component (in the denominator) of L [Eqs. (1) and (3)] is a function of u^1. Therefore, while increases in wind speed result in increases in both shear and buoyant production of turbulence, with all other factors held constant, increases in shear production dominate.

Grossman (1982) found that rolls dominated over cellular convection when $-z_i/L$ was less than 21.4. In general, estimation of z_i is difficult. However, Kristovich (1991) found a reasonable correspondence between the height at which the radar reflectivity decreased to half of the within-boundary layer values and aircraft in situ observations of the top of the boundary layer. An examination of the vertical variation of radar reflectivity from *CP3* and *CP4* indicated that between 1300 and

1700 UTC, the boundary layer depth remained at about 1100 m (not shown). Just prior to the time when rolls were most dominant, 1500–1600 UTC, $-z_i/L$ reached its minimum of about 40. This suggests that rolls were most favored following frontal passage.

c. Temporal changes of wind profiles

While estimates of surface heat and momentum fluxes are useful indicators of when rolls are favored, wind profiles are needed to determine mechanisms responsible for roll development and for comparison with existing theories on the importance of shear to the development and maintenance of rolls. Three datasets were available on 17 December 1983 for examining temporal changes in wind profiles. Radar dual-Doppler observations gave useful information on mean wind profiles, but lack data within the lowest regions of the boundary layer. Aircraft observations, taken during ascents and descents from Muskegon Airport, could be combined with research rawinsonde observations, taken at 1031 and 1606 UTC at the airport. However, lack of many soundings and large scatter in the data make these inadequate to examine details of the temporal evolution of the wind profiles during the entire observational time period. Winds derived by the velocity–azimuth display (VAD) method have high vertical and temporal resolution of wind profiles, but have the disadvantage of being averaged over an increasing large circle of radar observations with increasing height. Aerial changes in wind velocity would influence the mean wind obtained at each height by this technique. Indeed, examination of winds used in this method show a general decrease in wind speed as the air passed from the lake to the land surface, as expected. However, the influence of these wind variations on the calculated wind velocities, particularly at low levels within the boundary layer, appeared to be small. In addition, because of the shallow nature of the boundary layer on 17 December 1983, radar observations utilized for this study were limited to those within a 16-km range. VAD wind profiles were calculated for each radar sweep during this case, and were compared, where possible, with profiles from aircraft and rawinsonde observations.

VAD estimates of wind velocity profiles when rolls were dominant (1502 UTC) and when the convection was more cellular (1751 UTC) are given in Fig. 11. The wind speed and direction estimates above 500 m agreed reasonably well with dual-Doppler estimates for those levels over water (not shown). However, the influences of differences in surface friction between the lake and land areas are obvious: VAD estimates of wind speed below 500 m are less than aircraft observations (see Fig. 9). In general, wind speeds decreased throughout the depth of the boundary layer as the convection became more cellular. Variations were much greater in the lower half of the boundary layer, where wind speeds decreased by 2–4 m s^{-1}. Wind shear changes with time were greatest below about 200-m height, even with the observed underestimates of wind speed at low levels. A slight backing in wind direction, from about 280° to 270°, was observed between these time periods, but there were little or no changes in directional wind shear. Taken

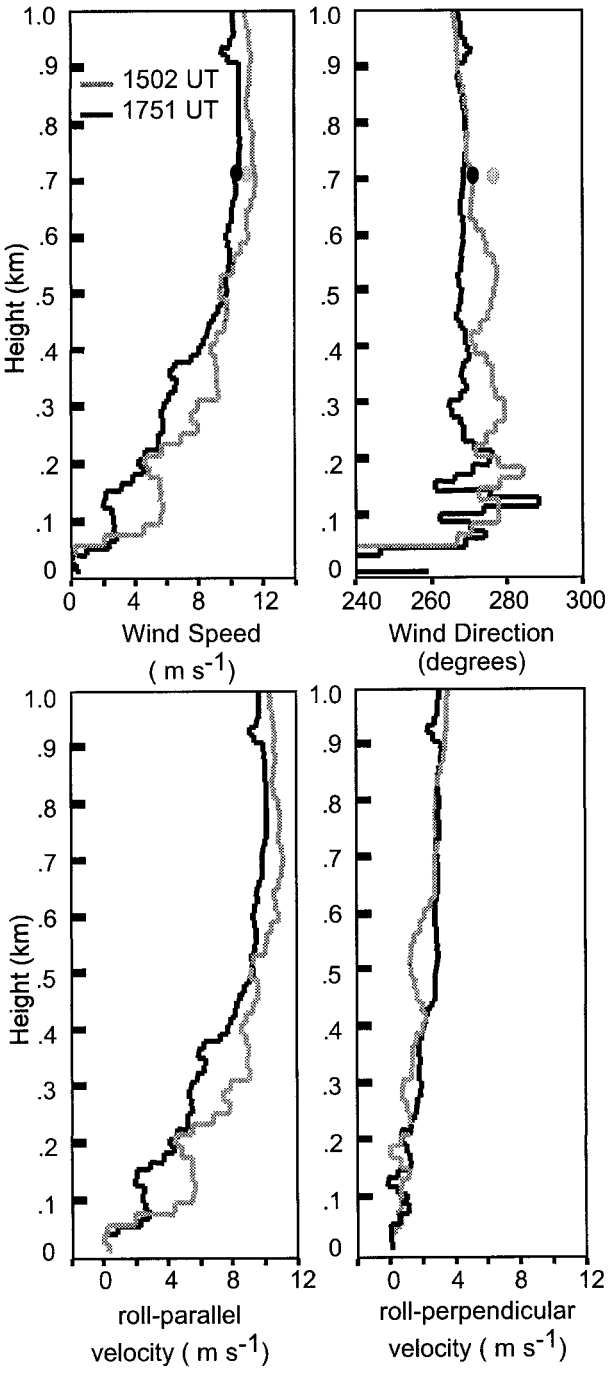

FIG. 11. Wind speed and direction profiles derived from VAD methods at 1502 and 1751 UTC on 17 Dec 1983. Dual-Doppler estimates at 0.7-km height are shown by shaded dots. Components of the wind velocity are given relative to the roll angle between 1500 and 1600 UTC, for reference.

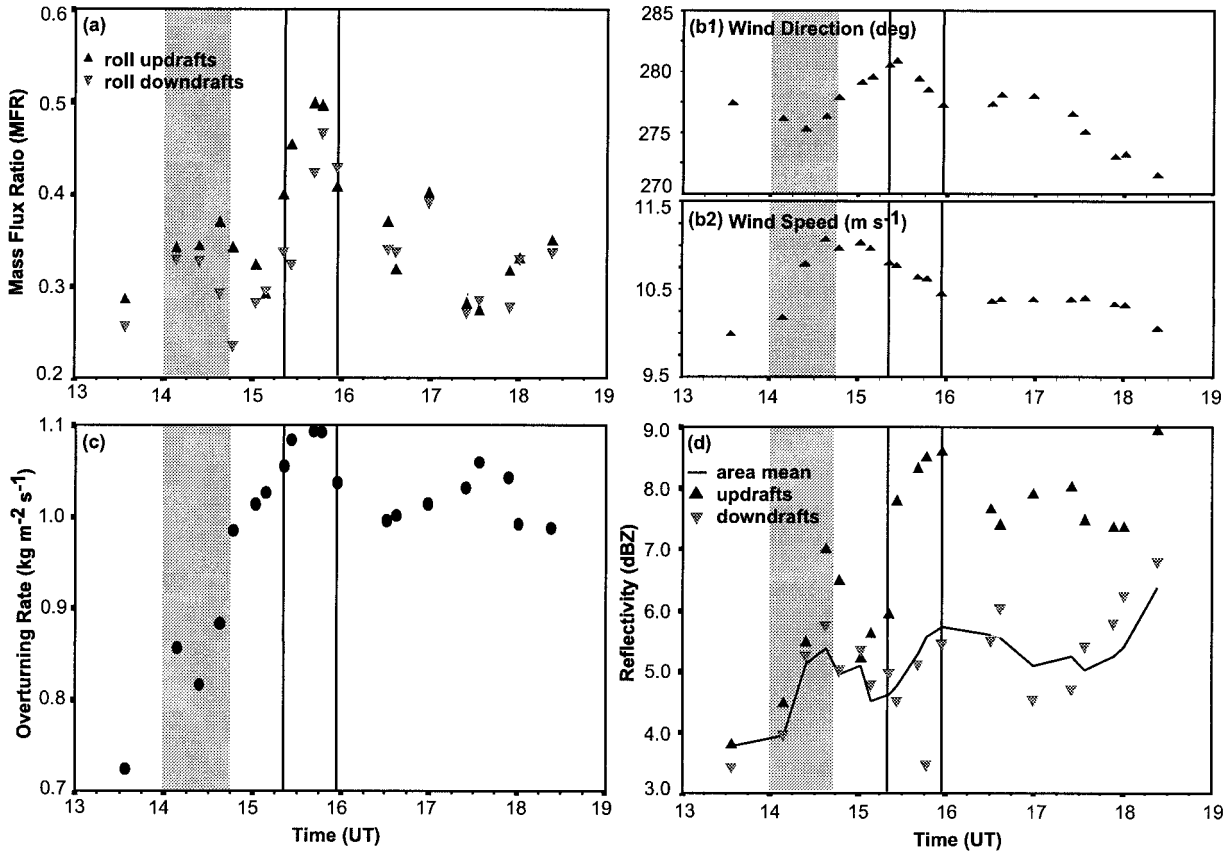

FIG. 12. Time series of (a) MFR, (b1) wind direction and speed, (c) mass overturning rate (sum of both updraft and downdraft mass fluxes), and (d) radar effective reflectivity factor at 700-m height within the dual-Doppler observational field. Radar reflectivity values are also shown for all grid points with verticle motions calculated as positive (filled triangles, updraft) and negative (open triangles, downdraft).

together, these variations suggest that differences in low-level wind speed and shear may have played a significant role in the transition of convection from roll to more cellular convection during this time period.

VAD observations suggest that, particularly at low levels, wind shear was greater during and just before the time when rolls became dominant in the overlake convective field. Surface wind observations support that the timing of these changes occurred within about an hour of changes in the convective field. Variations in wind speed shear tended to be higher, and more consistent, than variations in directional shear, giving support for mechanisms favoring speed shear forced roll convection in this case (e.g., Kuettner 1959, 1971; Sykes and Henn 1989; Kristovich 1993; Weckwerth et al. 1993).

7. Temporal changes of boundary layer overturning and radar reflectivity

A limited number of studies have suggested that the magnitude of vertical motions may change during transitions of convective structures within the boundary layer. For example, Braham (1986) found that the snowfall rate, derived from radar reflectivity measurements, decreased markedly during a time period when cellular convection dominated, and was much higher when linear patterns were present.

To determine how the boundary layer may respond to changes in the convective structure between roll and cellular convection, we examined changes in convective strength and snowfall rate on 17 December 1983 (e.g., Braham 1986; Rao and Agee 1996). Figure 12 gives time series of wind speed, MFR, mean radar reflectivity, and mean overturning rate (sum of updrafts and downdrafts) at 700-m height within the dual-Doppler radar observational area. As noted in the previous section, wind speeds reached a maxima at around 1430 to 1500 UTC, with linear patterns becoming most prevalent (MFR highest) between about 1530 and 1600 UTC.

Throughout the time period from 1300 to 1700 UTC, mean reflectivity tended to increase slowly. As expected, when rolls became dominant, there was a large difference in radar reflectivity between regions of updraft and downdraft. After the time period of maximum roll activity, reflectivity gradually became more similar between updraft and downdraft regions. It was thought that this may be related to changes in the rate at which

updrafts and downdrafts traverse the boundary layer. Indeed, the mass overturning rate was highest during the time period of strongest roll convection. After 1600 UTC, when rolls became less coherent, the mass overturning rate decreased by only about 10%.

Scatterplots showing the relationship between the midlevel mass overturning rate, MFR, and mean wind speed at 700 m (not shown), reveal the close relationship between each of these variables. However, the time lag between the maximum wind speed at all levels and increases in linearity and the mass overturning rate makes the relationship less obvious. Computer-animated radar reflectivity patterns on this, and other dates, suggests that roll convective patterns, and conditions necessary for rolls, developed upstream of the sample region and then evolved across the lake into the sample region from the west-northwest. This, and the time lag of up to an hour between wind speed increases and roll observations on this case, may suggest either that the convection takes time to react to this forcing or that the convection is organized upstream of the sample area and subsequently advected in.

8. Discussion

While it is well known that roll structures are pervasive in the boundary layer, it has long been recognized that roll structures, particularly in boundary layers heated from below, usually have organized convective elements along the roll axes. For example, Kuettner (1971) described satellite signatures of roll circulations as a ''string of pearls,'' with each ''pearl'' describing a convective element along the roll. Past studies often give a range of conditions in which both rolls and cellular convective structures have been observed (such as Grossman 1982; Woodcock 1940). Our observations, and those of several past authors, suggest that the transition between roll convection and cellular convection is a gradual process, with possibly complex interactions between the rolls and cellular convection along them.

This study documents the degree of cellularity along roll axes using the reflectivity field to calculate the HAR (Weckwerth et al. 1997) and by developing the MFR, which is a measure of the fraction of vertical motions that can be attributed to roll circulations. Data availability and quality, as well as the phenomena of interest, should largely determine which method (HAR or MFR) will be most illuminating for future studies. In this study, we observe the evolution of the convective pattern on 17 December 1983 between primarily cellular patterns (MFR from 0.24 to 0.40, HAR from 1 to 5) to situations where roll circulations dominate (MFR near 0.5, HAR above 6). The changes in coherent circulations are reflected in recognizable changes in the horizontal structure of the snowfall patterns from primarily nonroll to one dominated by wind-parallel bands. These changes in convective pattern reveal interchanges between roll kinetic energy and cellular kinetic energy, which are accompanied by observed changes in atmospheric conditions.

To better understand the changes in atmospheric conditions that gave rise to the observed transitions between roll and cellular convective structures, changes in factors thought to control the development of rolls were examined for 17 December 1983. Temporal trends in surface fluxes provided important information about changes in surface forcing, despite limitations in the methods used (i.e., fluxes were derived from bulk estimates using surface observations over land, rather than over the lake, and assumed a minimum lake surface temperature, 0°C). Rolls dominated near and just after time periods when both surface heat fluxes (both latent and sensible) and boundary layer wind speeds were a maximum, suggesting that magnitudes of shear were sufficient to overcome the tendency for surface heating to favor cellular convection.

Both radar and aircraft wind profiles reveal that the greatest wind shear was below about $0.2z_i$. Variations of wind profiles with high temporal and vertical resolution are only available from radar measurements using VAD methods with data collected at radar sites near the downwind shore of Lake Michigan. The measured winds utilized were entirely over land for most of the lower half of the boundary layer, but some portions of the radar sweep at higher altitudes were over water. The wind profile underwent the largest change in the lower half of the boundary layer (particularly below about 400 m–$0.35z_i$) during periods of convective structure changes. Changes in both wind shear and wind speed were greatest in the layer below $0.2z_i$, with only minor variations in wind direction throughout the boundary layer depth. These results lend support to recent findings suggesting that low-level wind speed or alongroll wind shear (Kristovich 1993; Weckwerth et al. 1997) are responsible for the transitions between cellular and roll convective structures.

It is important to note that the development of roll convection occurred up to 1 h subsequent to the time period of maximum wind speed and surface fluxes (cf. Figs. 12a and 12b2). In addition, linear convective patterns did not develop in the sample region, but developed into the region from the northwest. These observations suggest either the roll structures require a spinup time for development following optimum conditions or that the conditions that initiated the rolls occurred over the upwind half of Lake Michigan. With the current dataset, it is not possible to determine if rolls developed over the upwind half of the lake and advected into the sample region, or if the necessary conditions for rolls moved across the lake and into the region. Numerical modeling efforts and improved observations are required to determine if unique conditions near the upwind shore of the Great Lakes (such as rapid changes in surface friction and surface heating rates) are responsible for the development of rolls over the lakes, and may explain why rolls over Lake Michigan often occur in

conditions that are predicted by past studies to favor cellular convection (Kristovich 1993). New observational data taken during the 1997–98 field operations of the Lake-Induced Convection Experiment (Kristovich et al. 1998), and associated numerical modeling efforts, are under study to give information on convective evolution over the upwind half of Lake Michigan.

Braham (1986) found that time periods on 21 January 1984 when cellular convection dominated were accompanied by minimum snowfall rates. To examine this further, the current study investigated the evolution of the convective overturning and snowfall rates during transitions in boundary layer convective structure. Overall, average snowfall rates slowly increased throughout the day, with little correlation to convective structure or surface flux rates. The snowfall was more uniform when rolls were not present. Large differences in snowfall rate between updraft and downdraft areas were found when rolls were most dominant. The mean mass overturning rate within the boundary layer, on scales of km^2, maximized at the time periods when roll structures were most dominant (MFR highest), rather than when the highest surface fluxes and wind speeds were observed. This may suggest either a delay in the response of the boundary layer to surface heating, or may indicate that roll circulations are more efficient at vertical mixing than nonroll convective structures. Further studies of the east–west evolution of vertical mixing rate and convective structure may give insight into this surprising finding.

Acknowledgments. This research was sponsored by collaborative Grants NSF ATM 95-10098 (Illinois State Water Survey) and NSF ATM 95-10011 (South Dakota School of Mines and Technology). Reviews by Nancy Westcott (ISWS), Bruce Rose (University of Illinois in Urbana–Champaign), Tammy Weckwerth (National Center for Atmospheric Research), and anonymous reviewers greatly improved the text. The assistance by L. J. Miller (NCAR) with VAD radar analyses is appreciated.

REFERENCES

Arya, S. P., 1988: *Introduction to Micrometeorology.* Academic Press, 307 pp.

Asai, T., 1970: Stability of a plane parallel flow with variable vertical shear and unstable stratification. *J. Meteor. Soc. Japan,* **48,** 129–138.

——, 1972: Thermal instability of a shear flow turning the direction with height. *J. Meteor. Soc. Japan,* **50,** 525–532.

Atkinson, B. W., and J. W. Zhang, 1996: Mesoscale shallow convection in the atmosphere. *Rev. Geophys.,* **34,** 403–431.

Braham, R. R., Jr., 1986: Cloud and motion fields in open cell convection over Lake Michigan. Preprints, *23d Conf. on Radar Meteorology and Conf. on Cloud Physics,* Snowmass, CO, Amer. Meteor. Soc., JP202–JP205.

——, and M. J. Dungey, 1984: Quantitative estimates of the effect of Lake Michigan on snowfall. *J. Climate Appl. Meteor.,* **23,** 940–949.

——, and ——, 1995: Lake-effect snowfall over Lake Michigan. *J. Appl. Meteor.,* **34,** 1009–1019.

——, and D. A. R. Kristovich, 1996: On calculating the buoyancy of convective cores. *J. Atmos. Sci.,* **53,** 654–658.

Brown, R. A., 1970: A secondary flow model for the planetary boundary layer. *J. Atmos. Sci.,* **27,** 742–757.

——, 1972: On the inflection point instability of a stratified Ekman boundary layer. *J. Atmos. Sci.,* **29,** 850–859.

——, 1980: Longitudinal instabilities and secondary flows in the planetary boundary layer: A review. *Rev. Geophys. Space Phys.,* **18,** 683–697.

Brummer, B., 1985: Structure, dynamics and energetics of boundary layer rolls from KonTur aircraft observations. *Beitr. Phys. Atmos.,* **58,** 237–254.

Chang, S., and R. R. Braham Jr., 1991: Observational study of the development of a snow producing convective internal boundary layer over Lake Michigan. *J. Atmos. Sci.,* **48,** 2265–2279.

Clark, T. L., T. Hauf, and J. P. Kuettner, 1986: Convectively forced internal gravity waves: Results from two-dimensional numerical experiments. *Quart. J. Roy. Meteor. Soc.,* **112,** 899–925.

Cooper, K. A., 1998: Numerical simulations of convective rolls and cells in lake-effect snow bands. M.S. thesis, Dept. of Atmospheric Sciences, South Dakota School of Mines and Technology, 128 pp. [Available from Department of Atmospheric Sciences, South Dakota School of Mines and Technology, 501 E. St. Joseph St., Rapid City, SD 57701.]

Eichenlaub, V. L., 1979: *Weather and Climate of the Great Lakes Region.* University of Notre Dame Press, 335 pp.

Etling, D., and R. A. Brown, 1993: Roll vortices in the planetary boundary layer: A review. *Bound.-Layer Meteor.,* **65,** 215–248.

Garratt, J. R., 1992: *The Atmospheric Boundary Layer.* Cambridge University Press, 316 pp.

Grossman, R. L., 1982: An analysis of vertical velocity spectra obtained in the BOMEX fair-weather, trade-wind boundary layer. *Bound.-Layer Meteor.,* **23,** 323–357.

Hauf, T., and T. L. Clark, 1989: Three-dimensional numerical experiments on convectively forced internal gravity waves. *Quart. J. Roy. Meteor. Soc.,* **115,** 309–333.

Kelly, R. E., 1977: The onset and development of Rayleigh–Benard convection in shear flows: A review. *Physicochemical Hydrodynamics,* D. B. Spalding, Ed., Advance Publications, 65–79.

Kelly, R. D., 1984: Horizontal roll and boundary layer interrelationships over Lake Michigan. *J. Atmos. Sci.,* **41,** 1816–1826.

——, 1986: Mesoscale frequencies and seasonal snow falls for different types of Lake Michigan snow storms. *J. Climate Appl. Meteor.,* **25,** 308–321.

Kristovich, D. A. R., 1991: The three-dimensional flow fields of boundary layer rolls observed during lake-effect snow storms. Ph.D. thesis, University of Chicago, 178 pp. [Available from University of Chicago, 5801 S. Ellis, Chicago, IL 60637.]

——, 1993: Mean circulations of boundary-layer rolls in lake-effect snow storms. *Bound.-Layer Meteor.,* **63,** 293–315.

——, and R. Steve, 1995: Lake-effect cloud band frequencies over the Great Lakes. *J. Appl. Meteor.,* **34,** 2083–2090.

——, and R. R. Braham Jr., 1998: Mean profiles of moisture fluxes in snow-filled boundary layers. *Bound.-Layer Meteor.,* **87,** 195–215.

——, G. Young, J. H. Verlinde, P. Sousounis, P. Mourad, and D. Lenschow, 1998: The Lake-Induced Convection Experiment (Lake-ICE): A scientific overview and operational update. Preprints, *Second Conf. on Coastal Atmospheric and Oceanic Prediction,* Phoenix, AZ, Amer. Meteor. Soc., 34–37.

Kuettner, J. P., 1959: The band structure of the atmosphere. *Tellus,* **11,** 267–294.

——, 1971: Cloud bands in the earth's atmosphere—Observations and theory. *Tellus,* **23,** 404–425.

——, P. A. Hildebrand, and T. L. Clark, 1987: Convection waves: Observations of gravity wave systems over convectively active boundary layers. *Quart. J. Roy. Meteor. Soc.,* **113,** 445–467.

LeMone, M. A., 1973: The structure and dynamics of horizontal roll

vortices in the planetary boundary layer. *J. Atmos. Sci.,* **30,** 1077–1091.

——, 1976: Modulation of turbulence energy by longitudinal rolls in an unstable planetary boundary layer. *J. Atmos. Sci.,* **33,** 1308–1320.

——, and W. T. Pennell, 1976: The relationship of trade wind cumulus distribution to subcloud layer fluxes and structure. *Mon. Wea. Rev.,* **104,** 524–539.

Miller, L. J., C. G. Mohr, and A. J. Weinheimer, 1986: The simple rectification of Cartesian space of folded radial velocities from Doppler radar sampling. *J. Atmos. Oceanic Technol.,* **3,** 162–174.

Miner, T. J., and J. M. Fritsch, 1997: Lake-effect rain events. *Mon. Wea. Rev.,* **125,** 3231–3248.

Moeng, C.-H., and M. A. LeMone, 1995: Atmospheric planetary boundary-layer research in the US: 1991–1994. U.S. National Report to Int. Union of Geodesy and Geophysics 1991–1994, Amer. Geophys. Union, 1432 pp. [Available from American Geophysical Union, 2000 Florida Avenue, N. W., Washington, DC 20009-1277.]

Mohr, C. G., and R. L. Vaughn, 1979: An economical procedure for Cartesian interpolation and display of reflectivity data in three-dimensional space. *J. Appl. Meteor.,* **18,** 661–670.

——, L. J. Miller, R. L. Vaughn, and H. W. Frank, 1986: The merger of mesoscale datasets into a common Cartesian format for efficient and systematic analyses. *J. Atmos. Oceanic Technol.,* **3,** 144–161.

Muira, Y., 1986: Aspect ratios of longitudinal rolls and convection cells observed during cold air outbreaks. *J. Atmos. Sci.,* **43,** 26–39.

Rao, G.-S., and E. M. Agee, 1996: Large eddy simulation of turbulent flow in a marine convective boundary layer with snow. *J. Atmos. Sci.,* **53,** 86–100.

Schoenberger, L. M., 1986: Mesoscale features of the Michigan land breeze using PAM II temperature data. *Wea. Forecasting,* **1,** 127–135.

Scott, R. W., and F. A. Huff, 1996: Impacts of the Great Lakes on regional climate conditions. *J. Great Lakes Res.,* **22,** 845–863.

Steve, R. A., 1996: Evolution of convective elements in lake-effect boundary layers. M.S. thesis, Dept. of Atmospheric Sciences, University of Illinois in Urbana–Champaign, 67 pp. [Available from Department of Atmospheric Sciences, University of Illinois in Urbana–Champaign, 105 S. Gregory St., Urbana, IL 61801.]

Streten, N. A., 1975: Cloud cell size and pattern evolution in Arctic air advection over the North Pacific. *Arch. Meteor. Geophys. Bioklim.,* **24A,** 213–228.

Sykes, R. I., and D. S. Henn, 1989: Large-eddy simulations of turbulent sheared convection. *J. Atmos. Sci.,* **46,** 1106–1118.

——, W. S. Lewellen, and D. S. Henn, 1988: A numerical study of the development of cloud street spacing. *J. Atmos. Sci.,* **45,** 2556–2569.

——, D. S. Henn, and W. S. Lewellen, 1993: Surface-layer description under free-convection conditions. *Quart. J. Roy. Meteor. Soc.,* **119,** 409–421.

Weckwerth, T. M., J. W. Wilson, R. M. Wakimoto, and N. A. Crook, 1997: Horizontal convective rolls: Determining the environmental conditions supporting their existence and characteristics. *Mon. Wea. Rev.,* **125,** 505–526.

Wilson, J. W., T. M. Weckwerth, J. Vivekanandan, R. M. Wakimoto, and R. W. Russel, 1994: Boundary layer clear-air echoes: Origins of echoes and accuracy of derived winds. *J. Atmos. Oceanic Technol.,* **11,** 1184–1206.

Woodcock, A. H., 1940: Convection and soaring over the open sea. *J. Mar. Res.,* **3,** 3248–3253.